

# Highly Integrated Ultra-Compact Three-Port Converter Systems for Automotive Applications

Jannik Schäfer, *Student Member, IEEE*, and Johann W. Kolar, *Fellow, IEEE*

**Abstract**—Due to the enormous cost pressure in the development of automotive power electronic systems, a high degree of integration on a system level and cost-effective production of the individual power components are an absolute must in order to develop competitive products. This means that only converter topologies can be considered that use the built-in power components as efficiently as possible, but at the same time only require components that can be manufactured in a particularly cost-effective way. Such a topology is introduced in the following, which uses a single transformer to enable power flow between three isolated voltage buses, which are commonly found in today's electric vehicles (the output of a non-isolated single-phase PFC rectifier, the high-voltage battery, and the low-voltage battery). The presented three-port DC/DC converter topology is particularly cheap to implement in hardware, since all magnetic components can be built with PCB-integrated windings, which makes them more cost-effective to manufacture than conventional wire-wound windings. Furthermore, to use PCB-winding inductors efficiently, the so-called compensating fringing-field concept is employed, which allows for reducing the high-frequency conduction losses of PCB-windings significantly. The performance of the topology is finally verified by means of a 3.6 kW 500 V/500 V/15 V hardware demonstrator, which achieves a peak efficiency of 96.6% at a power density of  $16.4 \text{ kW L}^{-1}$ .

**T**HE exponential growth of the global electric vehicle (EV) market over the past few decades has created a new, very lucrative market for manufacturers of power electronic systems. Due to the high sales figures, however, the number of providers has increased continuously, which has led to enormous cost pressure on the development of automotive power electronics. For this reason, it is essential to optimize the entire power distribution network in an EV, as well as the individual power electronic systems down to the component level in terms of component utilization and minimization of manufacturing costs. Only in this way can competitive products be developed and successfully launched on the market.

The typical power distribution network of today's EVs consists, amongst others, of two galvanically isolated converter systems (see **Fig. 1a**), with a 3 kW DC/DC converter supplying the low-voltage network with energy from the high-voltage battery while driving, and the single-phase AC/DC converter being used to charge the high-voltage battery from the single-phase AC mains. However, this AC/DC converter is only used if no alternative is available since its low output power of 3.6 kW leads to excessively long charging times. Charging at fast charging stations from the three-phase grid is therefore usually preferred, which is why the on-board charger is only used very rarely.

Thus, the utilization of the DC/DC and the AC/DC system is suboptimal, as always only one of the systems is in operation while the other is inactive. In particular, the components of

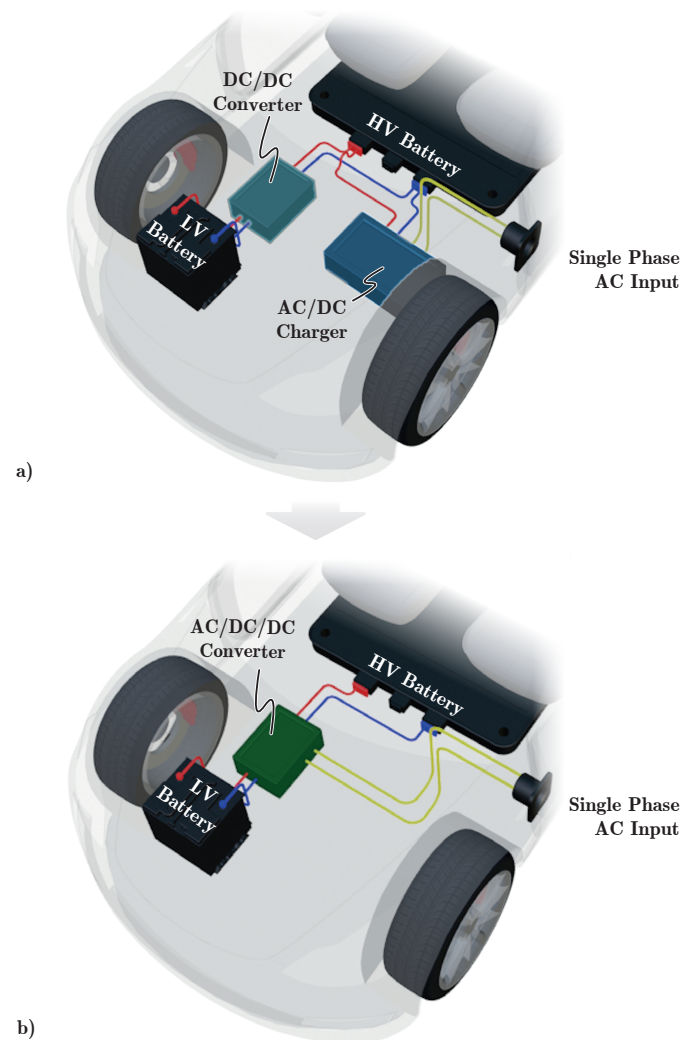


**Fig. 1.** a) Simplified power distribution grid in today's electric vehicles, where only the batteries, the isolated DC/DC converter and the isolated single-phase AC/DC charger are shown, and b) the integrated three-port AC/DC/DC converter with optimized component utilization.

the charger are very poorly utilized, as an expensive isolated 3.6 kW system must be installed, which, however, is hardly ever used. Fortunately, since both systems are rated for a similar output power (cf. **Tab. I**), the two subsystems can be integrated into a single three-port converter system, whereby the components of which are employed for both tasks and are

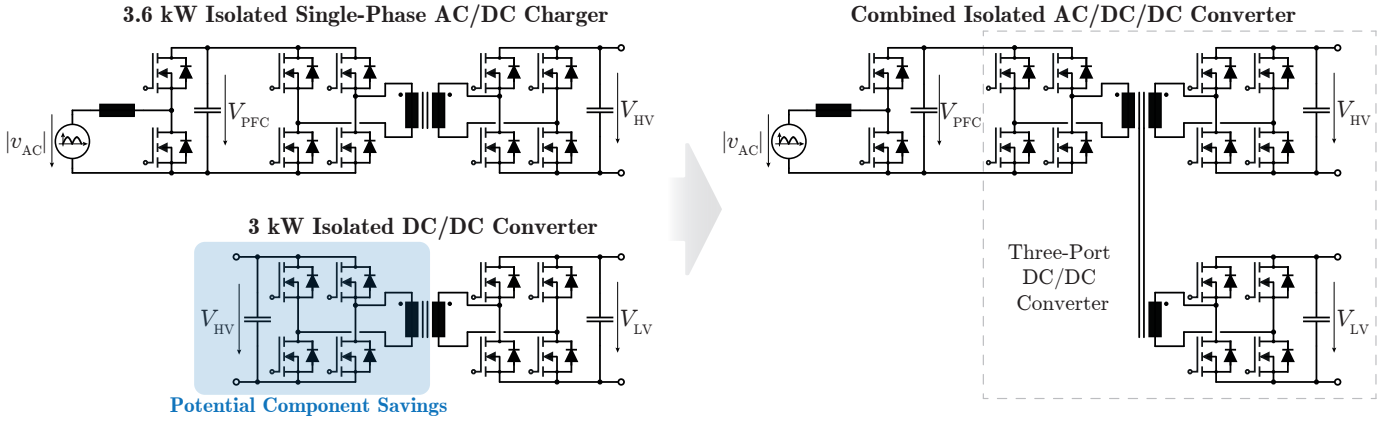


**Fig. 2.** Simplified schematic representation of the integration of the two subsystems, i.e. DC/DC converters into a single three-port converter, whereby for the sake of clarity, simple conventional topologies (dual-active-bridge converters) have been used as a basis for the considerations.

therefore used more effectively.

By means of such integration and the use of a suitable three-port converter topology, a complete 3.6 kW transformer and, depending on the original topology, up to four high-voltage power semiconductors can be saved without having to accept any reduction in functionality. This is shown schematically in **Fig. 2** based on simple conventional converter topologies. However, the resulting DC/DC three-port topology, the triple active bridge (TAB), is not ideal for the application at hand, since the wide voltage ranges at the different converter ports make a compact and cost-effective implementation of the transformer almost impossible. One of the reasons for this is that, considering costs, all magnetic components should be designed with PCB-integrated windings, which means that the expensive wire-wrapping process in the course of manufacturing these components can be avoided. However, since there is only little copper cross-section available in a PCB, the existing copper must be used as efficiently as possible, which means that the number of turns  $N$  must be minimized, as well as any current displacements due to high-frequency (HF) effects (skin and proximity effect) need to be reduced as far as possible. Thus, neither large magnetizing inductances ( $L_m \propto N^2$ ) nor large leakage inductances ( $L_\sigma \propto \int H_W^2 dV_W$ ) can be realized in compact and efficient PCB-winding transformers, as large leakage inductances can only be realized with either large winding volumes  $V_W$ , or strong magnetic fields  $H_W$  within the winding window, which, however, have a negative impact on the HF winding losses.

#### Isolated Single-Phase AC/DC Charger

Input Voltage Range:	70...272 $V_{rms}$
Input Current (max.):	16 $A_{rms}$
Output Voltage Range:	250...500 V
Output Power:	3.6 kW

#### Isolated DC/DC Converter

Input Voltage Range:	250...500 V
Output Voltage Range:	10.5...15 V
Output Power:	3 kW/200 A

**TABLE I.** Specifications of the isolated charger and step-down converter systems.

This inevitably leads to the conclusion that PCB-winding magnetics are optimal for topologies with a low inductance requirement, which unfortunately does not apply to the TAB (cf. **Fig. 2**) with its need for large leakage inductances [1]. However, to compensate for the variable port voltage differences due to the state-of-charge-dependent battery voltages ( $V_{LV}$ ,  $V_{HV}$ ), a certain inductance is absolutely necessary between the converter ports, which is used to control the power flow between the batteries. As the leakage inductance of PCB-winding transformers is not large enough, discrete PCB-winding inductors must be used that employ the compensating fringing-field concept (CFFC) [2]. This concept uses the  $y$ -component of an existing fringing field  $H_{ag}$  around an air gap to partially compensate the  $y$ -component of the parasitic skin and proximity fields  $H_{prox}$  and thereby minimizes the HF losses in the winding (cf. **Fig. 3**). Furthermore, by using appropriate cooling strategies for the PCB winding, current densities of up to  $100 A mm^{-2}$  are feasible in the PCB, without running into thermal issues (cf. **Fig. 4**). This means that efficient and compact HF PCB-winding inductors can be designed, but their reasonably achievable inductance values are still limited due to the small copper cross-sectional area in PCBs and the resulting upper limit on the number of turns. Accordingly, a three-port converter topology is in demand,

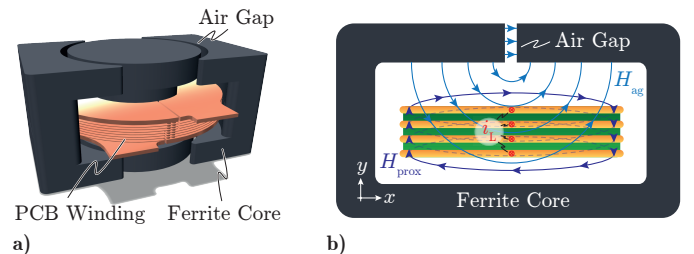


**Fig. 3.** a) 3D model of an exemplary CFFC PCB-winding inductor with two turns and b) simplified representation of the field distributions in a cross-section of the winding window of a PCB-winding inductor with four turns, that uses the compensating fringing-field concept (CFFC), where the fringing field  $H_{ag}$  around the air gap partially compensates the parasitic proximity field  $H_{prox}$  and therefore ensures a more equal current distribution and/or a relatively low AC winding resistance.

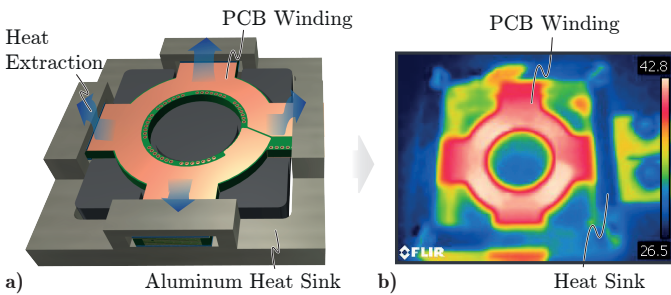


**Fig. 4.** a) 3D model of an exemplary CFFC PCB-winding inductor with four thermal cooling interfaces and b) the corresponding thermal image of the current-carrying PCB winding (without the ferrite core), which is thermally connected to a water-cooled heat sink.

which allows operation with very small stray inductances of the transformer and only requires discrete inductors with small inductances, whereby the windings of all magnetic components can efficiently be integrated into the PCB. This reduces the manufacturing costs of the magnetic components to a minimum.

Since the non-isolated AC/DC PFC rectifier front-end is anyway required and is topologically not affected by the integration of the two subsystems, only the isolated three-port DC/DC converter is investigated in more detail in the following. One possible three-port DC/DC converter topology is shown in **Fig. 5**, which requires PCB-winding magnetics only and can therefore be manufactured at low costs [3]. The topology basically consists of two functional groups, since the power flow between the PFC port ( $V_{PFC}$ ) and the HV port ( $V_{HV}$ ) is via a series-resonant converter, while the LV port draws its required energy via two parallel step-down converters either from the PFC port in charging mode, where the car is connected to the single-phase AC mains, or from the HV port in driving mode.

The series-resonant converter part is operated as a DC transformer, which means that the output voltage follows the input voltage directly and the converter is operated with a voltage transfer ratio corresponding to the turns ratio of the transformer. The output voltage at the HV port is therefore

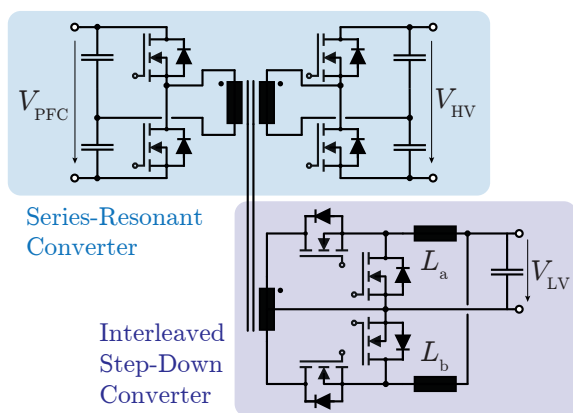


**Fig. 5.** General circuit structure of the isolated three-port DC/DC converter with a series-resonant converter part between the PFC rectifier port and the HV port and an interleaved step-down converter part which is connected to the LV port of the transformer.

indirectly controlled by means of the output voltage of the upstream PFC rectifier ( $V_{PFC}$ ). This has the advantage that a minimal leakage inductance in the transformer is already sufficient to operate the resonant converter efficiently. In addition, the currents in the transformer are almost sinusoidal, which means that the HF conduction losses can be minimized. Furthermore, as there is hardly any control required, it is possible to operate the converter with a constant duty cycle of 50%, whereby the split DC-link capacitors can be used as resonant capacitors and the number of semiconductors can therefore be halved.

Besides the power flow from the PFC port to the HV port, there is simultaneously a small power flow from the HV port to the LV port required, which charges the small LV battery if necessary. However, due to the operation of the series-resonant converter part, a rectangular voltage is inherently induced in the LV winding of the three-winding transformer, the excursion of which is given by the HV voltage, scaled down by means of the turns ratio. However, this induced voltage does not automatically correspond to the required output voltage of the LV port, which is why this voltage must be adapted using the two interleaved step-down converters.

The positively induced voltage-time areas are used as the input voltage for the step-down converter with the output inductance  $L_a$ , while the negative voltage-time areas are used for the second step-down converter with the inductance  $L_b$ . As a result, the two step-down converters are automatically operated with a phase shift of 180° and can be operated with a maximum duty-cycle of 50% (cf. **Fig. 6**).

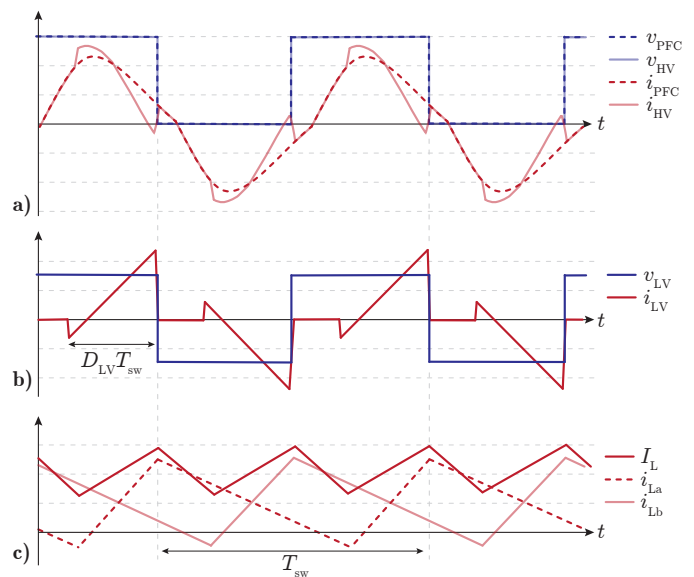


**Fig. 6.** Simplified exemplary waveforms of the three-port DC/DC converter in charge mode operation, where equal numbers of turns of the PFC and the HV windings are assumed. In a)  $v_{PFC}$ ,  $v_{HV}$ ,  $i_{PFC}$  and  $i_{HV}$  denote the PFC side winding voltage, the HV side winding voltage, the PFC winding current and the HV winding current, respectively. In b)  $v_{LV}$ ,  $i_{LV}$  and  $D_{LV} T_{sw}$  denote the LV side winding voltage, the LV winding current and the duty cycle of the two step-down converters, whereas in c)  $I_L$ ,  $i_{La}$  and  $i_{Lb}$  denote the sum of the LV inductor currents, the current in  $L_a$  and the current in  $L_b$ , respectively.

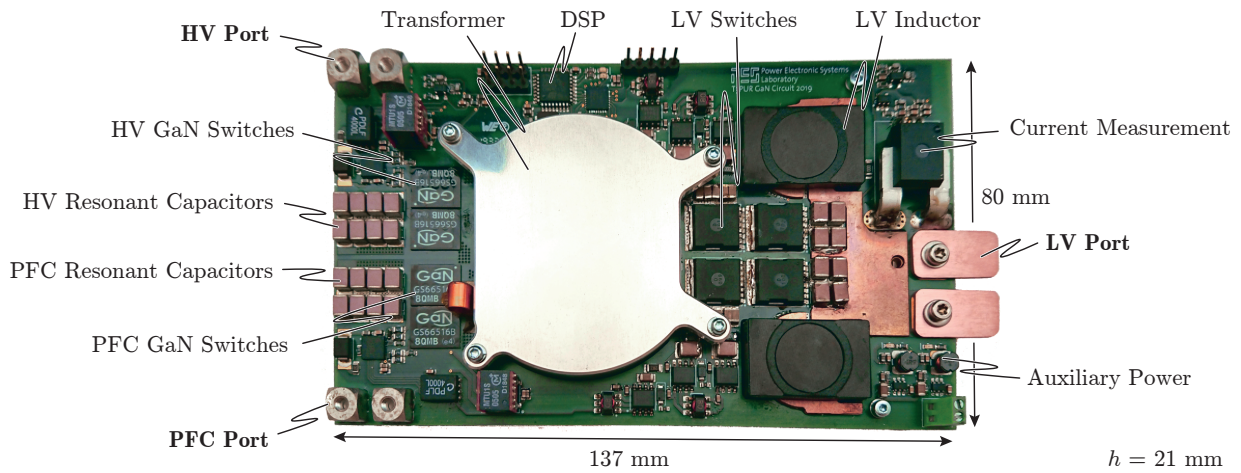


**Fig. 7.** Hardware prototype of the 3.6 kW three-port DC/DC converter system with a total height of  $h = 21$  mm (including the volume of the water-cooled heat sink).

Hence, in charge mode operation, the HV port voltage is mainly controlled by means of the PFC rectifier output voltage  $V_{PFC}$ , while the LV port output voltage is controlled by means of the duty cycles of the interleaved step-down converters of the LV port.

In drive mode operation, the converter is operated in the same way, but as there is only power flow between the HV port and the LV port required, the resonant converter is not operated, which means that the switching frequency no longer has to correspond to the resonant frequency and can therefore be used as an additional control parameter to optimize the efficiency of the power conversion.

In order to investigate the performance of this topology experimentally, a 3.6 kW hardware demonstrator with a power density of  $16.4 \text{ kW L}^{-1}$  was developed, which can cover the

entire required voltage ranges of the different converter ports (cf. **Tab. I**). In this prototype, only PCB-winding magnetics are used, making the manufacturing process of the entire converter system extremely cost-effective. In the PFC port and the HV port, there are two  $650 \text{ V}/25 \text{ m}\Omega$  GaN switches used for each half-bridge, while inexpensive silicon MOSFETs are used in the LV port [4]. Instead of the currently relatively expensive GaN switches, cheaper SiC switches can also be used in the PFC port and the HV port, without a noticeable deterioration in performance. The efficiency of the hardware demonstrator is shown in **Fig. 8** for different operating points. Even though the system is very compact and simple, a remarkable efficiency can be achieved for the most important operating points, which are full power ( $P_{\text{out}} = 3.6 \text{ kW}/V_{\text{HV}} = 500 \text{ V}/V_{\text{LV}} = 14.5 \text{ V}$ ) in charge mode and partial power ( $P_{\text{out}} = 1.5 \text{ kW}/V_{\text{HV}} = 500 \text{ V}/V_{\text{LV}} = 14.5 \text{ V}$ ) in drive mode.

## CONCLUSION

The proposed three-port DC/DC converter topology, in combination with the compensating fringing-field concept (CFFC) for PCB-winding inductors, enables a very compact and inexpensive implementation of a power electronic system for electric vehicles, which can be used to provide multiple galvanically isolated paths for the power flow between the high-voltage battery, the low-voltage battery and the output of an upstream non-isolated PFC rectifier. Despite the high power density of  $16.4 \text{ kW L}^{-1}$  of the 3.6 kW hardware demonstrator, a relatively high peak efficiency of 96.6% is achieved.

## REFERENCES

- [1] C. Zhao, S. D. Round, and J. W. Kolar, "An isolated three-port bidirectional dc-dc converter with decoupled power flow management," *IEEE Transactions on Power Electronics*, vol. 23, no. 5, pp. 2443–2453, 2008.
- [2] J. Schäfer, D. Bortis, and J. W. Kolar, "Novel highly efficient/compact automotive pcb winding inductors based on the compensating air-gap fringing field concept," *IEEE Transactions on Power Electronics*, vol. 35, no. 9, pp. 9617–9631, 2020.
- [3] J. Schäfer and J. W. Kolar, "Three-port series-resonant dc/dc converter for automotive charging applications," *Electronics*, vol. 10, no. 20, p. 2543, 2021.
- [4] J. Schäfer, "Highly integrated ultra-compact three-port converter systems for automotive applications," Ph.D. dissertation, ETH Zurich, 2020.

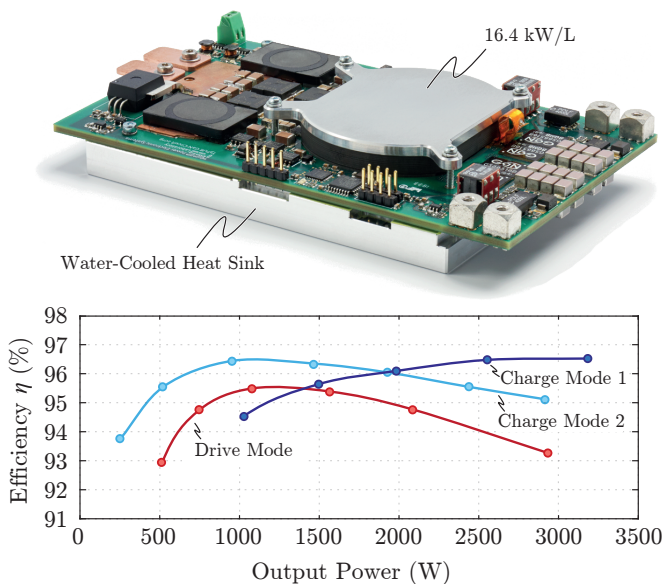


**Fig. 8.** Experimental measurement results of the 3.6 kW three-port DC/DC converter prototype for  $V_{\text{HV}} = 500 \text{ V}/V_{\text{LV}} = 14.5 \text{ V}$  in "Charge Mode 1",  $V_{\text{HV}} = 250 \text{ V}/V_{\text{LV}} = 14.5 \text{ V}$  in "Charge Mode 2", and  $V_{\text{HV}} = 500 \text{ V}/V_{\text{LV}} = 14.5 \text{ V}$  in "Drive Mode".